Journal of Sound and Vibration 329 (2010) 3348–3358

Contents lists available at ScienceDirect

Journal of Sound and Vibration

journal homepage: www.elsevier.com/locate/jsvi

Prediction of uncertain frequency response function bounds using polynomial chaos expansion

A. Manan, J.E. Cooper *

Department of Engineering University of Liverpool Liverpool, L69 7EF, UK

ARTICLE INFO

Article history:
Received 4 February 2009
Received in revised form
9 November 2009
Accepted 6 January 2010
Handling editor: A.V. Metrikine
Available online 26 March 2010

ABSTRACT

A probabilistic method is developed to predict the uncertainty bounds on Frequency Response Functions (FRFs) developed from Finite Element models. A non-intrusive Polynomial Chaos Expansion (PCE) method is used to predict uncertainty regression models of the various parameters that make up a curvefit of the FRF: natural frequencies, damping ratios, complex amplitudes, mass and stiffness residuals, by making use of an efficient Latin Hypercube technique. These uncertainty models are then combined to efficiently determine PDFs of the parameters and also the uncertainty bounds of the FRFs. The approach is demonstrated using two examples; a simple beam containing uncertainty in Young's Modulus, and a full-scale aircraft composite wing model containing uncertainties in both Young's modulus and the shear modulus. The results were compared with Monte Carlo Simulation (MCS) and it was found that the parameter PDFs and FRF error bounds obtained using a 2nd-order PCE model agreed very well whilst requiring significantly less computation.

1. Introduction

Cost competitive, high quality and low lead time product demands are requirements for a wide range of engineering products requiring accurate modelling techniques. However, unknown physical properties at the design phase and production design tolerances or inaccuracies introduce variability and uncertainties into the in-service response of the structure or product. For such real life problems, the deterministic approach has proved inadequate for design quality assessment and hence there has been the need to explore probabilistic or non-probabilistic approaches. The case considered here is the prediction of the bounds of the Frequency Response Function (FRF) of a given structure. The most straightforward technique to explore the effect of uncertainties such as material properties and size tolerances is Monte Carlo simulation, however, in a wide number of applications the amount of computation required to give meaningful results is excessive. Consequently, there is a growing need to produce reliable and robust models that incorporate uncertainties and can predict the effect of uncertainty in a range of parameters in an efficient manner.

Uncertainties [1] can be handled using several theories, such as Probability Theory [2], Fuzzy Theory [3], Evidence Theory (also known as Dempster–Shafer Theory) [4,5], Bayesian Theory and Convex Model Theory [6,7]. Information gap decision theory under severe uncertainty has been also devised [8]. The common issue among these theories is how to determine the degree to which uncertain events are likely to occur, and there are distinct differences between the various approaches theories as to how this is achieved.

* Corresponding author.
E-mail address: j.e.cooper@liverpool.ac.uk (J.E. Cooper).

0022-460X/$ - see front matter © 2010 Elsevier Ltd. All rights reserved.
doi:10.1016/j.jsv.2010.01.008

Nomenclature

a_{i_1}, $a_{i_1 i_2}$ ...	deterministic coefficients of Hermite polynomials
$[C]$	damping matrix
H	frequency Response Function
H_f	fitted Frequency Response Function
j	$\sqrt{-1}$
$[K]$, k	global/element stiffness matrix
L	beam element length
$[M]$, m	global/element mass matrix
m_L	mass per unit length
n	number of modes
p	order of Hermite polynomial
β_i	deterministic coefficients
δ_{ij}	kronecker delta
$\psi_i\,(\xi(\theta))$	set of multidimensional Hermite polynomial
σ_x	standard deviation of random variable χ
χ	gaussian distributed random variable
χ_{mean}	mean of random variable χ
μ	mean value
σ	standard deviation
ω_i	frequency of mode i
ζ_i	damping ratio of mode i
$\xi_{i_1}(\theta)$	set of independent standard Gaussian random variables
$\Gamma_p[\xi_{i_1}(\theta)\ldots\xi_{i_p}(\theta)]$	set of multidimensional Hermite polynomials of order p.

Some investigation has been undertaken into the influence of uncertainties on FRFs [9,10], the focus to this work. The hybrid finite element method has been developed to predict the FRF bounds with interval or fuzzy uncertainties [9]. An approach which is based on sensitivity of the eigen properties to the structural modifications such as mass and stiffness distribution has been proposed to predict frequency, damping ratio and mode shapes from experimental modal testing [11]. Similarly, a method for damage detection within a beam is predicted by examining the difference of the imaginary part of the FRF before and after damage [12].

Developments of probabilistic models are possible via direct use of the stochastic expansion through either the Karhunen–Loeve (KL) [13] or Polynomial Chaos Expansions (PCE). In the KL expansion, truncated KL series are used to represent the random field and can be implemented in the Finite Element Model, and either perturbation theory or a Neuman expansion can be applied to determine the response variability.

Polynomial Chaos Expansion (PCE) is a method that has been used to explore the variability in flutter/divergence and gust response [14,15], control [16,17], computational fluid dynamics [18,19] and buckling problems [20]. The work of Choi et al. [20] provides the first application of a least squares-based hybrid approach using a Latin Hypercube sampling (LHS) technique [25] applied in a non-intrusive way to predict uncertainty in the critical buckling loads of a metallic joined wing structure subject to variations in Young's modulus. Five locations on the wing were selected to apply the uncertainty and an ANOVA (ANalysis Of VAriance) approach was used to find the dominant PCE polynomial coefficients.

The PCE approach is simple to implement when determining the response model and also does not require knowledge of the random process covariance function. The use of PCE has been found to be an efficient method even when other techniques such as Lyapunov's method have failed [16]. The potential of PCE is tremendous because of its simplicity, versatility and computational efficiency within the framework of Probability Theory. Most PCE applications explore the effect of random variables on some single response parameter such as flutter speed [15], critical buckling load [20] or control stability, performance and robustness [16,17].

In this work, the approach developed in [20] is extended to efficiently determine the confidence bounds of FRFs in mechanical systems containing uncertainty. Rather than having to determine a PCE model for every frequency line of the FRF, a system identification procedure is employed for each Latin Hypercube test case so that the FRF is represented by a limited number of parameters (natural frequency, damping ratio, complex amplitude, mass and stiffness residuals). PCE models of each parameter are then collectively placed into the FRF mathematical description to build a PCE–FRF model that can be used to predict the FRF bounds in an efficient manner.

The approach is demonstrated using FRFs generated by two examples. The first is a very simplistic metallic FE beam model with uncertainty in Young's modulus. The second case is a more realistic composite wing FE model with uncertainty in both Young's modulus and the shear modulus. Comparison of the predicted FRF bounds using the PCE approach is made with Monte Carlo simulations and it is shown that good agreement is found for a substantially lower computational effort.

2. Mathematical model formulation of deterministic frequency response function (FRF)

The equations of motion of a multi-degree of freedom vibration system can be modelled in the classical form [21] for response y to input force f as

$$[M]\ddot{\underline{y}}+[C]\dot{\underline{y}}+[K]\underline{y}=\underline{f} \tag{1}$$

where $[M]$, $[C]$ and $[K]$ are the mass, damping and stiffness matrices, respectively.

The solution of the homogenous form of Eq. (1) can be used to determine the natural frequencies, damping ratios and corresponding mode shapes. However, assuming a harmonic input and response, the Frequency Response Function matrix

H between sinusoidal forcing function f at frequency ω and output y is found as [21]

$$y(\omega)=H(\omega)f(\omega) \tag{2}$$

where the FRF matrix is defined as

$$H(\omega)=[K+i\omega C-\omega^2 M]^{-1} \tag{3}$$

It is common practice to fit the FRF between each input and output for the first n dominant modes in the form

$$H_f(\omega)\cong\sum_{i=1}^{n}\frac{A_i}{\omega_i^2-\omega^2+2j\zeta_i\omega_i\omega}+A_r+\frac{B_r}{\omega^2} \tag{4}$$

in which A_i are the complex residues, and A_r and B_r are mass and stiffness residuals, respectively and $H_f(\omega)$ is the fitted FRF. It is usual to perform a two stage procedure to identify the above model, firstly the frequencies and damping ratios are calculated either from the eigen solution of the system Eq. (3) or by using a curve-fitting technique such as the Rational Fraction Polynomial method [22] applied to measured input–output data. Then a linear curve fit is performed on Eq. (4) in order to determine the residual and residue coefficients.

3. Stochastic modelling

Norbert Wiener introduced a mathematical model of Brownian motion using a multiple stochastic integral with homogeneous chaos [23]. Subsequently, Ito modified Weiner's work [24] and showed that any stochastic processes can be described as a Weiner process. Irregularities due to parameter variations can be described mathematically as a PCE expansion. Ghanem and Spanos [13] introduced a simple definition of the PCE as a convergent series of the form [20]

$$u(\theta)=a_0\Gamma_0+\sum_{i_1=1}^{\infty}a_{i_1}\Gamma_1(\xi_{i_1}(\theta))+\sum_{i_1=1}^{\infty}\sum_{i_2=1}^{i_1}a_{i_1i_2}\Gamma_2[\xi_{i_1}(\theta),\xi_{i_2}(\theta)]+\sum_{i_1=1}^{\infty}\sum_{i_2=1}^{i_1}\sum_{i_3=1}^{i_2}a_{i_1i_2i_3}\Gamma_3[\xi_{i_1}(\theta),\xi_{i_2}(\theta),\ \xi_{i_3}(\theta)]+\ldots \tag{5}$$

where $\{\xi_{i_1}(\theta)\}_1^{\infty}$ is a set of independent standard Gaussian random variables, $\Gamma_p[\xi_{i_1}(\theta)\ldots\xi_{i_p}(\theta)]$ is a set of multidimensional Hermite polynomials of order p, $a_{i_1}a_{i_1i_2}\ldots$ are deterministic coefficients and θ is the random character of the quantities involved. The general expression for a multidimensional Hermite polynomial is given by [20]

$$\Gamma_p[\xi_{i_1}(\theta)\ldots\xi_{i_p}(\theta)]=(-1)^n\frac{\partial^n e^{-\frac{1}{2}\xi^T\xi}}{\partial\xi_{i_1}(\theta)\ldots\partial\xi_{i_p}(\theta)} \tag{6}$$

where vector ξ consists of n Gaussian random variables.

Simplifying Eq. (5) leads to

$$u(\theta)=\sum_{0}^{p}\beta_i\psi_i(\xi(\theta)) \tag{7}$$

in which β_i and $\psi_i(\xi(\theta))$ are identical to $a_{i_1},a_{i_1i_2}\ldots$ and $\Gamma_p[\xi_{i_1}(\theta)\ldots\xi_{i_p}(\theta)]$, respectively.

Consider the one dimensional Polynomial Chaos model; we can expand the random response u using orthogonal polynomials in ξ, which have a known probability distribution, for example say, unit normal. Now, if u is a function of Gaussian distributed random variable χ whose mean is χ_{mean} and variance $\sigma_\chi{}^2$, then ξ is the normalized variable

$$\xi=\frac{\chi-\chi_{\mathrm{mean}}}{\sigma_\chi} \tag{8}$$

Hence the response in one dimension can be expressed as

$$u=\beta_0+\beta_1\xi+\beta_2(\xi^2-1)+\beta_3(\xi^3-3\xi)+\beta_4(\xi^4-6\xi^2+3)+\ldots \tag{9}$$

where the orthogonal polynomials and $\xi(\theta)$ satisfy the following conditions:

$$\begin{gathered}\psi_0=1,\ \ \langle\psi_i\rangle=0,\ \ \langle\psi_i\psi_j\rangle=\langle\psi_i^2\rangle\delta_{ij}\ \ \forall i,j\\ \langle\xi^0\rangle=1,\ \ \langle\xi^{\mathrm{k}}\rangle=0,\ \ \forall\,k\text{ odd and }\langle\xi^{\mathrm{k}}\rangle=(\mathrm{k}-1)\langle\xi^{\mathrm{k}-2}\rangle\end{gathered} \tag{10}$$

with $\langle.\rangle$ indicating the expected value operation. The β_i terms are unknown coefficients that have to be calculated using computed test data sets. For the case that we are considering here, the u parameter is the natural frequency, damping ratio, complex amplitude, phase or the residuals, and the ξ variable might be the value of longitudinal Young's modulus or shear modulus of the wing.

If we have two uncertain variables, for instance the longitudinal Young's modulus and shear modulus, then it is referred to as a 2-D Polynomial Chaos model. The order of the model is inferred from the power of ξ. Using Eq. (3), the expanded form for a 2-D Polynomial Chaos model in which ξ_1 and ξ_2 are uncertain parameters, can be written as

$$u_{2nd}=\beta_0+\beta_1\xi_1+\beta_2\xi_2+\beta_3(\xi_1^2-1)+\beta_4\xi_1\xi_2+\beta_5(\xi_2^2-1) \tag{11}$$

The complex amplitude PCE model can be expressed in terms of real and imaginary parts such that

$$u_{2nd} = \beta_{0r} + \beta_{1r}\xi_1 + \beta_{2r}\xi_2 + \beta_{3r}(\xi_1^2 - 1) + \beta_{4r}\xi_1\xi_2 + \beta_{5r}(\xi_2^2 - 1) + \ldots \\ j(\beta_{0i} + \beta_{1i}\xi_1 + \beta_{2i}\xi_2 + \beta_{3i}(\xi_1^2 - 1) + \beta_{4i}\xi_1\xi_2 + \beta_{5i}(\xi_2^2 - 1)) \tag{12}$$

This complex PCE model was converted to amplitude and phase by taking the magnitude and angle between the real and imaginary parts. Here β_{ir} are coefficients of the real part of PCE model and β_{ii} are coefficients of the imaginary part of the PCE model.

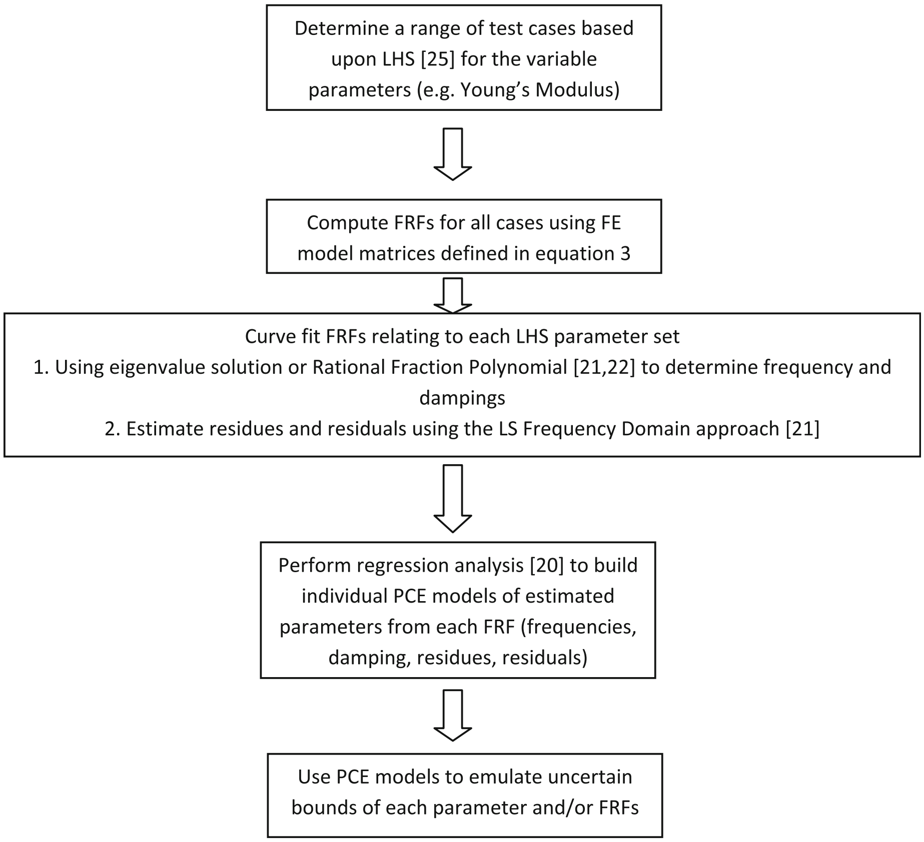

Fig. 1. Process to Determine PCE–FRF Models.

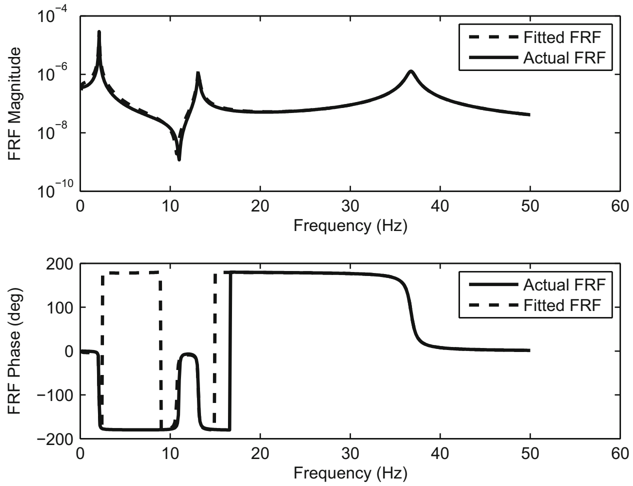

Fig. 2. Beam Model. Typical Fitted and Actual FRF plots.

4. Determination of PCE–FRF models

PCE regression models are developed by applying the uncertainty models in Section 3 to the FRF representation described in Section 2 as shown in Fig. 1.

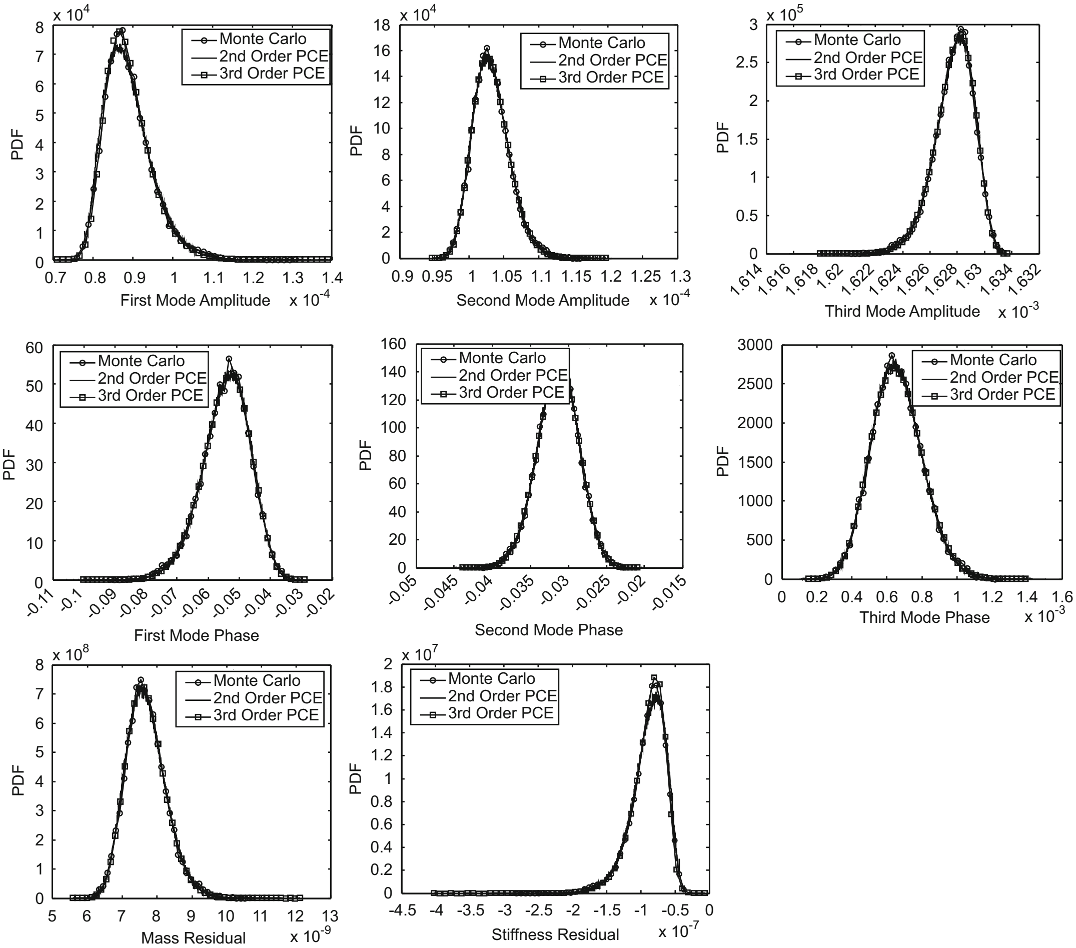

Fig. 3. Beam Model. PDF Distributions for Frequencies, Damping Ratios, Residue Amplitude and Phase and Mass and Stiffness Residual Distributions for first three modes using PCE and MCS.

Table 1
Cantilever Beam Model Statistics of Parameters using PCE and Monte Carlo methods.

Method	Mode 1				Mode 2				Mode 3			
	μ	σ	μ	σ	μ	σ	μ	σ	μ	σ	μ	σ
	Frequency (Hz)		**Damping**		**Frequency (Hz)**		**Damping**		**Frequency (Hz)**		**Damping**	
PCE	2.0931	0.0524	0.0083	1.744e−4	13.1180	0.3283	0.0053	7.271e−5	36.7388	0.9195	0.0120	2.780e−4
MCS	2.0931	0.0524	0.0083	1.748e−4	13.1179	0.3284	0.0053	7.269e−5	36.7387	0.9198	0.0120	2.781e−4
	Amplitude		**Phase**		**Amplitude**		**Phase**		**Amplitude**		**Phase**	
PCE	8.892e−5	5.863e−6	−0.0543	0.0077	1.032e−4	2.636e−6	−0.0314	0.0027	0.0016	1.456e−6	6.589e−4	1.461e−4
MCS	8.895e−5	5.991e−6	−0.0543	0.0077	1.032e−4	2.646e−6	−0.0314	0.0027	0.0016	1.462e−6	6.587e−4	1.454e−4
	Mass Residual		**Stiffness Residual**									
PCE	7.682e−9	5.688e−10	−8.897e−8	2.518e−8								
MCS	7.683e−9	5.720e−10	−8.912e−8	2.592e−8								

Statistics of Parameters using PCE and Monte Carlo methods.

For both cases considered in this paper Gaussian random variables have been used to model positive quantities. However, it is possible in other situations that should negative values occur, then the PCE might converge to an erroneous solution should numerical ill-conditioning occur, particularly if higher order expansions be needed. One approach to remedy this situation is to change the distribution of the uncertainty e.g. Lognormal, squared of a Gaussian or even uniform. This is an area for future study.

5. Simple beam model example

As a first example, a simple uniform beam finite element model which accounts for bending only in one plane (and without shear deformation or torsion) is developed to predict the dynamic response of a simple cantilever beam. The beam

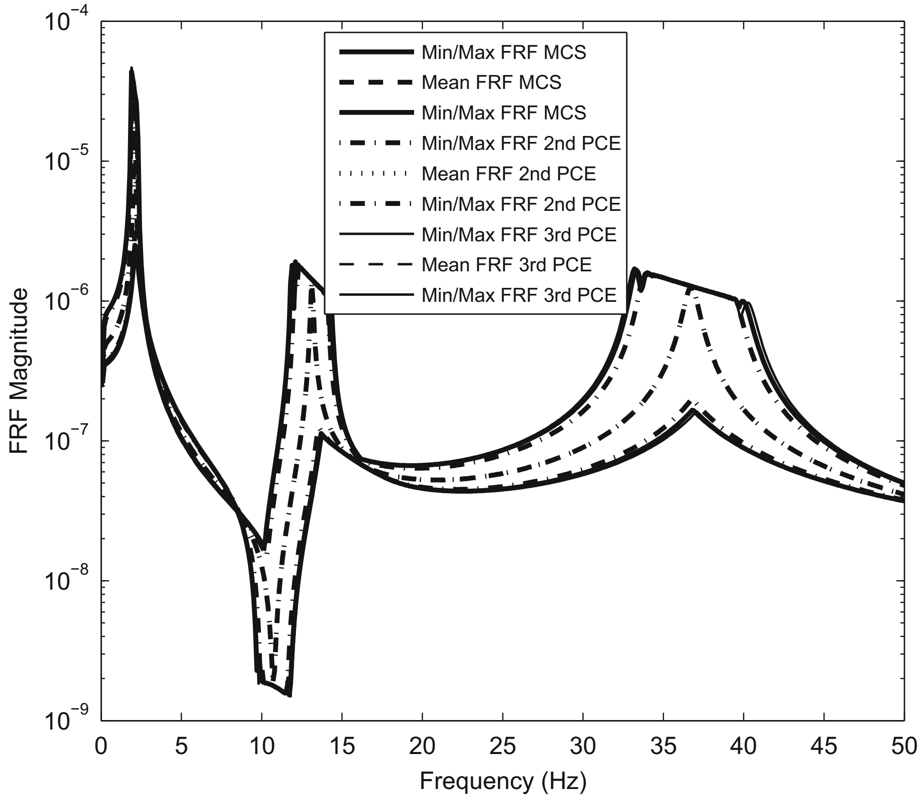

Fig. 4. Beam Model. FRF 99% Confidence Bounds by PCE and MCS approaches.

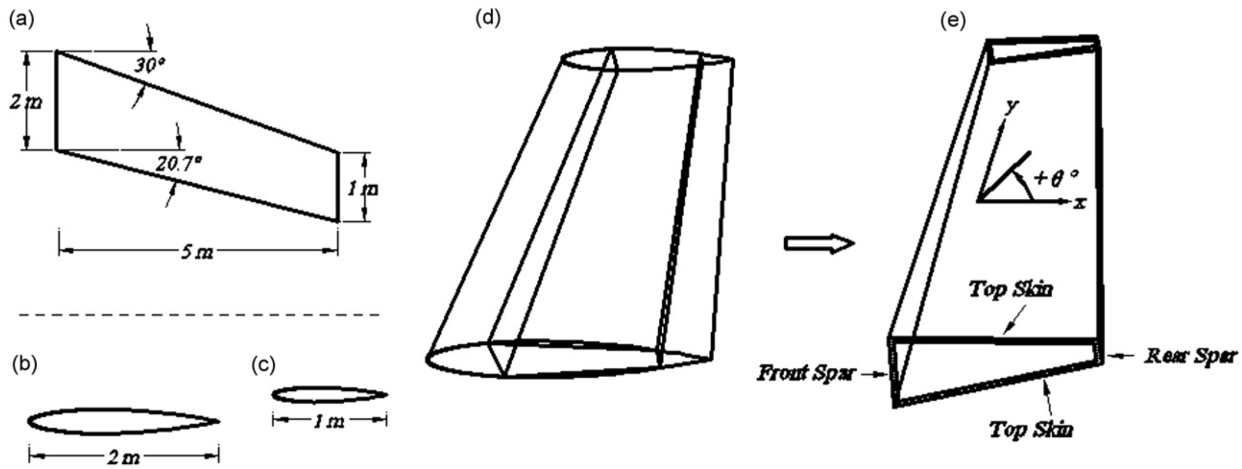

Fig. 5. Composite Wing Model Geometry.

element is expressed as a cubic polynomial which leads to the well-known expressions for the local element mass and stiffness matrices

$$m=\frac{m_L L}{420}\begin{bmatrix}156 & 22L & 54 & -13L\\ 22L & 4L^2 & 13L & -3L^2\\ 54 & 13L & 156 & -22L\\ -13L & -3L^2 & -22L & 4L^2\end{bmatrix},\quad k=\frac{EI}{L^3}\begin{bmatrix}12 & 6L & 12 & 6L\\ 6L & 4L^2 & -6L & 2L^2\\ -12 & -6L & 12 & -6L\\ 6L & 2L^2 & -6L & 4L^2\end{bmatrix} \tag{13}$$

where L is the element length, m_L is mass per unit length and EI is the flexural rigidity. A total of 10 elements were used to assemble the global mass and stiffness matrices, with proportional damping being introduced in the equation of motion in the usual manner such that

$$[C]=\alpha[M]+\beta[K] \tag{14}$$

where α and β were taken as 0.2 and 0.0001, respectively.

The deterministic FRF, obtained between two points of the simple cantilever FE model, is shown in Fig. 2 along with a typical curve fit. Note that the apparent large differences in the phase plot are erroneous and are due to the phase being plotted between $\pm 180^\circ$ so that, for example, -181° is plotted as 179°. This type of phase variation often occurs on commercial software and is not due to inaccuracies in the fitting process. A 1-D chaos model with variable Young's modulus of coefficient of variation of 0.05 was used to impart uncertainty into the model. A total of 15 Latin Hypercube Samples were taken to provide data for the second-order regression fit. PDF plots, as predicted by PCE model, for the first three frequencies and damping ratios are shown in Fig. 3 along with PDFs of the complex residues in terms of magnitude and phase, and also the residuals. To assess the quality of these PDFs, Monte Carlo Simulations were conducted with a total of 10,000 samples to construct equivalent PDFs. Excellent agreement is observed in each of the PDF plots for the various parameters as demonstrated with very similar mean and standard deviation results given in Table 1.

Based on these models, a PCE model for the FRF was developed by taking 15 Latin Hypercube samples across the entire frequency range. The FRF–PCE model was then emulated to predict 99% confidence bounds on the FRF, which were compared with 10,000 MCS results as shown in Fig. 4 for 2nd and 3rd-order PCE models. An excellent comparison was achieved for the mean values and also the upper and lower bounds. The similarities between the results for different order PCE models show that convergence has been achieved.

Table 2
Lay-up scheme and material properties for composite wing.

	Lay-up Scheme	Total Thickness (mm)	Material Properties	Value
Front Spar	$((-45^\circ)_4)_s$	1.00	E_1	140(GPa)
Rear Spar	$((-45^\circ)_4)_s$	1.00	E_2	10.0(GPa)
Top Skin	$((-45^\circ)_2$, $(45^\circ)_3$,$90)_s$	1.50	v	0.3
Bottom Skin	$((-45^\circ)_2$, $(45^\circ)_3$,$90)_s$	1.50	G_{12}	5.0(GPa)
Ribs	$((-45^\circ)_2)_s$	0.50	Ply thickness	0.125 (mm)
			Density	1570 (Kg/m^3)

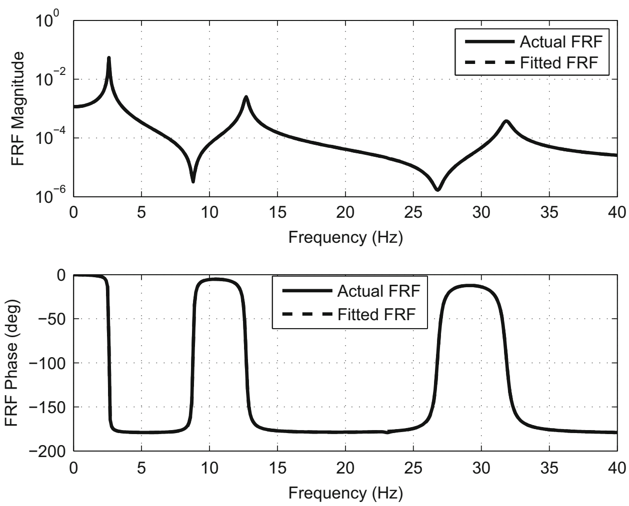

Fig. 6. Composite Wing Model. Typical Model and Fitted FRF Plots.

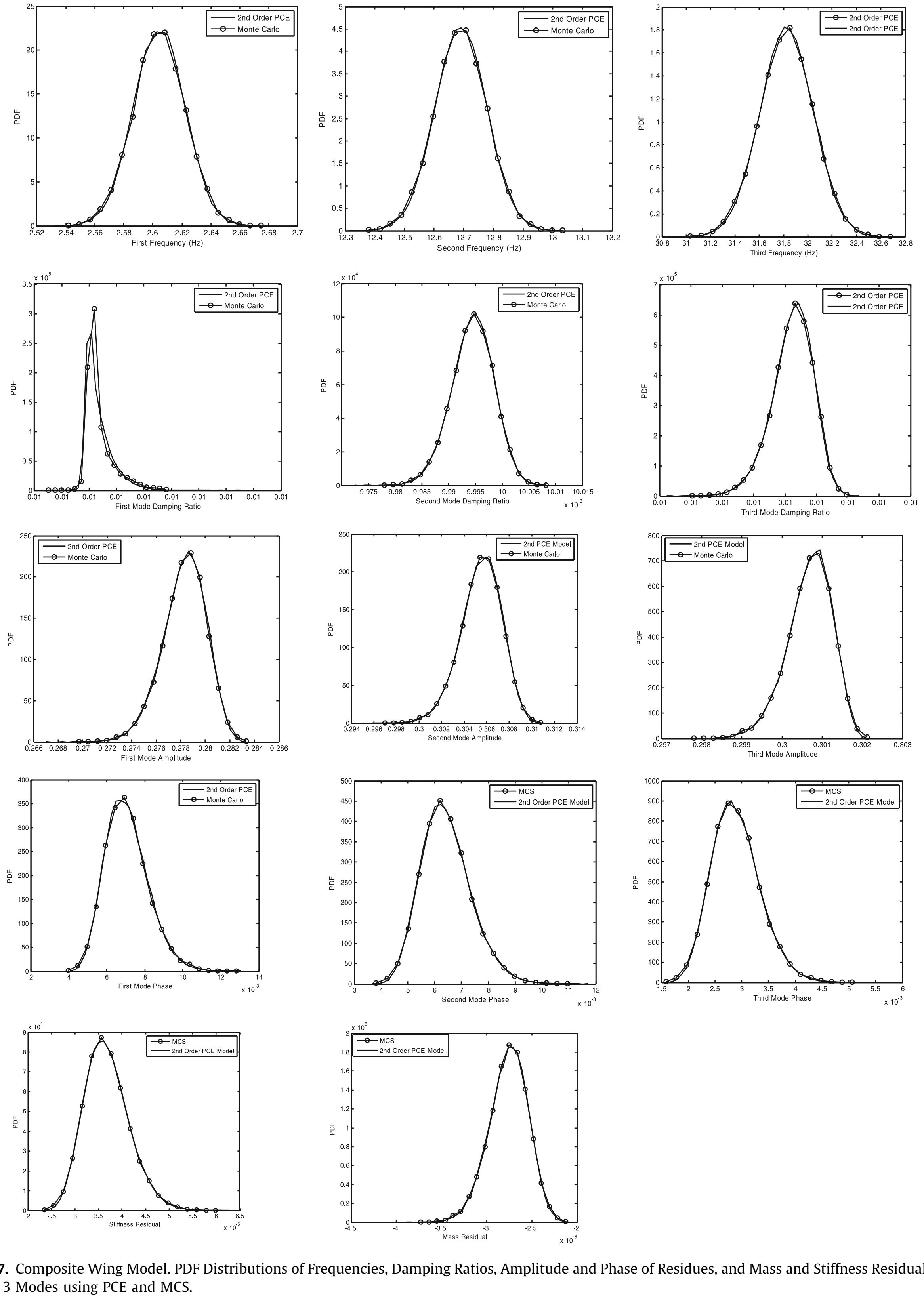

Fig. 7. Composite Wing Model. PDF Distributions of Frequencies, Damping Ratios, Amplitude and Phase of Residues, and Mass and Stiffness Residuals for First 3 Modes using PCE and MCS.

6 Composite wing example

As a more realistic test, the composite wing finite element model shown in Fig. 5 was implemented. The thickness-to-chord ratio for this wing is four percent and a geometrical box is fitted in it as a structural member that has front spar, rear spar, top skin and bottom. The torsion box was positioned such that its front spar lies at quarter chord and rear spar lies at the three quarter chord. Ten evenly spaced ribs were included to providing chord-wise stiffness to suppress local panel modes. Table 2 defines the lay-up orientation and material properties of the composite layers that were used.

A Finite Element Model of the wing was developed using NASTRAN with the FRF analysis performed assuming 2% structural damping. A typical FRF between the leading and trailing edge wing tips is shown in Fig. 6. Again the curve-fitting procedure gives good results.

Table 3
Composite Wing Model Statistics of Parameters using PCE and Monte Carlo methods.

Method	Mode 1				Mode 2				Mode 3			
	μ	σ	μ	σ	μ	σ	μ	σ	μ	σ	μ	σ
	Frequency (Hz)		**Damping**		**Frequency (Hz)**		**Damping**		**Frequency (Hz)**		**Damping**	
PCE	2.6043	0.0177	0.0100	2.5214e−6	12.6898	0.0874	0.0100	3.948e−6	31.8241	0.2195	0.0100	6.5887e−7
MCS	2.6043	0.0177	0.0100	2.5942e−6	12.6898	0.0878	0.0100	3.961e−6	31.8241	0.2204	0.0100	6.6126e−7
	Amplitude		**Phase**		**Amplitude**		**Phase**		**Amplitude**		**Phase**	
PCE	0.2783	0.0018	0.0071	0.0011	0.3055	0.0018	0.0064	9.221e−4	0.3007	5.5852e−4	0.0029	4.5186e−4
MCS	0.2783	0.0018	0.0071	0.0011	0.3055	0.0018	0.0064	9.263e−4	0.3007	5.6051e−4	0.0029	4.5381e−4
	Mass Residual		**Stiffness Residual**									
PCE	−2.759e−6	2.1453e−7	3.6785e−5	4.7319e−6								
MCS	−2.759e−6	2.1553e−7	3.6785e−5	4.7427e−6								

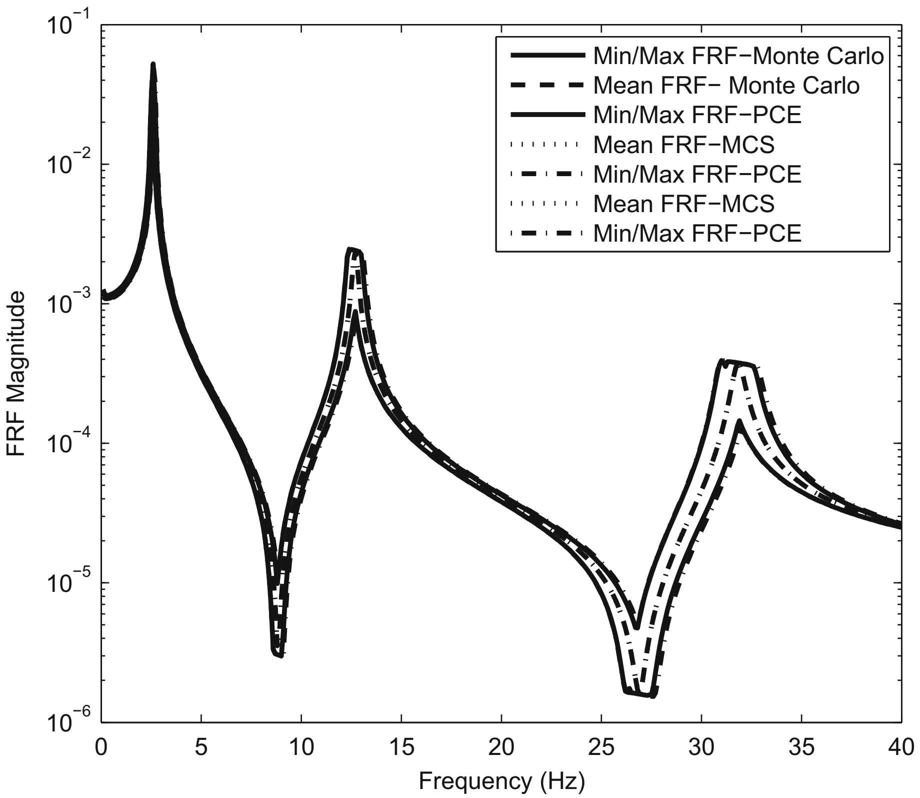

Fig. 8. Composite Wing Model. 95% FRF Confidence Bands FRF Plot by PCE and MCS approaches (E and G Uncertain parameters).

Table 4
Computational cost for both test cases.

Model Type	Method	Time(sec)
Beam	Monte Carlo Simulation (10 000)	2447
	PCE Approach	141
Composite Wing	Monte Carlo Simulation (10 000)	81277
	PCE Approach	697

A PCE model for FRF by taking 60 Latin Hypercube Samples was developed in which 2-D chaos was introduced via longitudinal Young's modulus and shear modulus of wing's spars, skins and ribs. Variation on the longitudinal Young's modulus was normal with mean of 140 GPa with standard deviation 2.8 GPa whereas that for the shear modulus was also normal with mean of 5.0 GPa with standard deviation 0.1 GPa. The FRF–PCE model was then emulated with 400 samples producing PDF plots which are shown in Fig. 7 for 2nd order models. A Monte Carlo Simulation was conducted with a total of 10,000 samples to assess the PDFs predicted using the PCE method and it can be seen that there is a good agreement, although it must be remembered that there are far fewer MCS calculations with this example which have resulted in a more disjointed amplitude behaviour of the MCS PDFs compared to the first example, but in all cases the frequency distribution is similar. Table 3 shows the excellent agreement between the mean and standard deviation for all of the individual modal parameters. Finally, when the individual PCE regression models are combined to give the FRF–PCE model, Fig. 8 shows that the FRF confidence bands have a very good agreement.

Table 4 shows the computational time required on a PC for both test cases using the Monte Carlo (full simulation and error bound computation) and PCE (LHS sampling and emulations) approaches. It can be seen that for the simple beam case, the PCE method requires 5.81% of the computation required for the MCS, whereas for the Composite wing FE model only 0.86% of the computation is required. These differences will get much greater as the complexity of the structural model increases.

7. Conclusions

In this paper, an approach to determine a probabilistic FRF model using the Polynomial Chaos Expansion (PCE) technique is described. PCE models are developed for the modal parameters determined from curve-fitting FRFs obtained from a Finite Element model using a Latin Hypercube technique to define the test cases. The individual probabilistic frequency, damping ratio and complex amplitude PCE models are then combined to define the probabilistic FRF–PCE model. The methodology is illustrated on a simple cantilever beam example with variation in Young's Modulus and also an aircraft composite wing FE model in which the longitudinal and shear modulus were allowed to vary. For considered cases, the PDF estimates using the PCE approach for the modal parameters, and also the overall FRF scatter bounds, compare very well with those obtained from extensive Monte Carlo simulations even though the PCE-based model is much more computationally efficient. Further work is required to assess the application of the method when much higher numbers of uncertain variables are included.

References

[1] A. Hunter, S. Parsons, *Applications of Uncertainty Formalisms*, Springer, New York, 1998, pp. 8–32.
[2] A.H.S. Ang, W.K. Tang, *Probability Concepts in Engineering Planning and Design, Vol. I and II, Basic Principles*, John Wiley and Sons, Inc., NY, 1984.
[3] K.L. Wood, K.N. Otto, E.K. Antonsson, Engineering design calculations with fuzzy parameters, *Fuzzy Sets and Systems* 52 (1992) 1–20.
[4] G. Shafer, *A Mathematical Theory of evidence*, Princeton University Press, Princeton, NJ, 1976.
[5] H. Bae, R.V. Grandhi, R.A. Canfield, An approximation approach for uncertainty quantification using evidence theory, *Reliability engineering and system safety* 86 (2004) 215–225.
[6] P. Soundappan, E. Nikolaidis, R.T. Haftka, R.V. Grandhi, R. Canfield, Comparison of evidence theory and Bayesian theory for uncertainty modelling, *Reliability Engineering and System Safety* 85 (2004) 295–311.
[7] Y. Ben-Haim, I. Elishakoff, *Convex Models of Uncertainty in Applied Mechanics*, Elsevier Science Publishers B.V, 1990.
[8] Y. Ben-Haim, *Information-gap Decision Theory: Decisions Under Severe Uncertainty*, Academic Press, 2001.
[9] M. De Munck., D. Moens., W. Desmet, D. Vandepetti, An adaptive Kriging based optimisation for interval and fuzzy FRF analysis., in: International conference of noise and vibration engineering Ketholieke Universitiet Leuven, Belgium (ISMA 2008) pp. 3767–3776.
[10] K. Mendrok, L. Pieczonka, T. Uhl, Assessment of uncertainty of experimentally obtained modal parameters, in: International conference of noise and vibration engineering Ketholieke Universitiet Leuven, Belgium (ISMA 2008) pp. 3899–3910.
[11] G. Coppotelli., On the estimate of FRFs from operational data, *Mechanical Systems and Signal Processing* 23 (2) (February 2009) 288–299.
[12] X. Liu, N.A.J. Lieven, P.J. Escamilla-Ambrosio, Frequency response function shape-based methods for structural damage localisation, Mechanical Systems and Signal Processing 23 (4) (2009) 1243–1259.
[13] R.G. Ghanem, P.D. Spanos, *Stochastic Finite Elements: A Spectral Approach*, Springer-Verlag, New York Inc., 1991.
[14] A. Manan, J.E. Cooper, Uncertainty of Composite Wing Aeroelastic Behaviour, 12th AIAA/ISSMO Multidisciplinary Analysis and Optimization Conference, Victoria, British Columbia, Sep. 10–12, 2008.
[15] A. Manan, J.E. Cooper, Design of Composite wing by including uncertainties: a probabilistic approach, *Journal of Aircraft* 46 (2) (2009) 601–607.
[16] F.S. Hover, M.S. Triantafyllou., Application of polynomial chaos in stability and control, *Automatica* 42 (2006) 789–795.
[17] A.H.C. Smith, Robust and Optimal Control using Polynomial Chaos Theory, Ph.D. thesis, University of South Carolina, 2007.

[18] L. Mathellin., M.Y. Hussaini, T.A. Zang., Stochastic approaches to uncertainty quantification in CFD simulations, *Numerical Algorithms* 38 (2005) 209–236.
[19] O.M. Knioa, O.P. Le Maître, Uncertainty propagation in CFD using polynomial chaos decomposition, *Journal of Fluid Dynamics Research* 38 (2006) 616–640.
[20] S.K. Choi, R.V. Grandhi, R.A. Canfield, C.L. Pettit, Polynomial chaos expansion with latin hypercube sampling for estimating response variability, *AIAA Journal* 42 (6) (June 2004) 1191–1198.
[21] D.J. Ewins, Modal Testing—Theory, Practice and Application, Research Studies Press Ltd.
[22] M.H. Richardson, D.L. Fermenti. Parameter Estimation From Frequency Response Measurements using Rational Fraction Polynomials, 1st IMAC conference, Orlando, Florida, November, 1982.
[23] N. Wiener, The Homogeneous Chaos, *American Journal of Mathematics* 60 (4) (October 1938) 897–936.
[24] K. Ito, Multiple wiener integrals, *Journal of Mathematical Society. Japan* 3 (1951) 157–169.
[25] M.D. Mckay., R.J. Beckman, W.J. Conover, A comparison of three methods for selecting values of input variables in the analysis of output from a computer code, *Technometrics* 21 (2) (May 1979) 239–245.